Molecular Pharmacology Fast Forward. Published on January 22, 2019 as DOI: 10.1124/mol.118.114769
This article has not been copyedited and formatted. The final version may differ from this version.

Chronic menthol does not change stoichiometry or functional plasma membrane levels of mouse α3β4-containing nicotinic acetylcholine receptors

Selvan Bavan, Charlene H. Kim, Brandon J. Henderson, Henry A. Lester

Division of Biology and Biological Engineering, California Institute of Technology, Pasadena, CA, USA (SB, CHK, HAL); Department of Biomedical Sciences, Joan C Edwards School of Medicine at Marshall University, Huntington, WV, USA (BJH).

Molecular Pharmacology Fast Forward. Published on January 22, 2019 as DOI: 10.1124/mol.118.114769
This article has not been copyedited and formatted. The final version may differ from this version.

Running title: α3β4 AChRs slightly modified by chronic menthol

Corresponding authors:

1) Selvan Bavan, 1200 East California Boulevard, Division of Biology and Biological Engineering, California Institute of Technology, Pasadena, CA 91125, USA.

Telephone number: 626 395 4946.

Fax number: 626 564 8709.

Email address: sbavan@caltech.edu

2) Henry A. Lester, 1200 East California Boulevard, Division of Biology and Biological Engineering, California Institute of Technology, Pasadena, CA 91125, USA.

Telephone number: 626 395 4946.

Fax number: 626 564 8709.

Email address: lester@caltech.edu

Number of text pages: 49

Number of tables: 3

Number of figures: 3

Number of references: 73

Words in Abstract: 249

Words in Introduction: 730

Words in Materials and Methods: 1693

Words in Discussion: 1492

Molecular Pharmacology Fast Forward. Published on January 22, 2019 as DOI: 10.1124/mol.118.114769
This article has not been copyedited and formatted. The final version may differ from this version.

Non-standard abbreviations: EMEM, Eagle's Minimum Essential Medium; ER, endoplasmic reticulum; ERES, endoplasmic reticulum exit site(s); GFP, green fluorescent protein; HeLa, human epithelial; HSD, honestly significant difference; IPN, interpeduncular; MhB, medial habenula; mOSm, milliosmoles; nAChR, nicotinic acetylcholine receptor; Neuro-2a, neuroblastoma-2a; PM, plasma membrane; Rs, series resistance; SNc, substantia nigra pars compacta; SNPs, single nucleotide polymorphisms; SNr, substantia nigra pars reticulata; V_m, membrane potential; VTA, ventral tegmental area; WT, wild-type; Zn^{2+} co-app., Zinc co-application.

Molecular Pharmacology Fast Forward. Published on January 22, 2019 as DOI: 10.1124/mol.118.114769
This article has not been copyedited and formatted. The final version may differ from this version.

Abstract

Heteromeric α3β4 nAChRs are pentameric ligand-gated cation channels that include at least two α3 and at least two β4 subunits. They have functions in peripheral tissue, peripheral and central nervous systems. We examined the effects of chronic treatment with menthol, a major flavor additive in tobacco cigarettes and in electronic nicotine delivery systems, on mouse α3β4 nAChRs transiently transfected into neuroblastoma 2a (Neuro-2a) cells. Chronic menthol treatment at 500 nM, near the estimated menthol concentration in the brain following cigarette smoking, altered neither the [ACh]-response relationship nor Zn^{2+} sensitivity of ACh-evoked currents, suggesting that menthol does not change α3β4 nAChR subunit stoichiometry. Chronic menthol treatment failed to change the current density (peak current amplitude/cell capacitance) of 100 μM ACh-evoked currents. Chronic menthol treatment accelerated desensitization of 100 μM and 200 μM ACh-evoked currents. Chronic nicotine treatment (250 μM) decreased ACh-induced currents, and we found no additional effect of including chronic menthol. These data contrast with previously reported, marked effects of chronic menthol on β2* nAChRs studied in the same expression system. Mechanistically, the data support the emerging interpretation that both chronic menthol and chronic nicotine act on nAChRs in the early exocytotic pathway, and that this pathway does not present a rate-limiting step to the export of α3β4 nAChRs; these nAChRs include endoplasmic reticulum (ER) export motifs but not ER retention motifs. Previous reports show that smoking mentholated cigarettes enhances tobacco addiction; but our results show that this effect is unlikely to arise via menthol actions on α3β4 nAChRs.

Molecular Pharmacology Fast Forward. Published on January 22, 2019 as DOI: 10.1124/mol.118.114769
This article has not been copyedited and formatted. The final version may differ from this version.

Introduction

Smoking is the leading cause of preventable death worldwide (CDC, 2018), and is responsible for ~6 million deaths annually (WHO, 2015). Nicotine causes smoking addiction through binding to pentameric ligand-gated nicotinic acetylcholine receptors (nAChRs). Chronic exposure to nM or μM concentrations causes upregulation of nAChRs at the plasma membrane (PM). This upregulation occurs partially because nicotine enters the endoplasmic reticulum (ER), binds there to nascent α4β2 nAChRs, acts as a posttranslational pharmacological chaperone for these nAChRs, and consequently increases ER exit of these nAChRs via posttranslational pharmacological chaperoning (Henderson and Lester, 2015; Srinivasan et al., 2012b). Nicotine upregulates nAChR α4 or β2 protein levels without changing their mRNA levels (Buisson and Bertrand, 2001; Flores et al., 1992; Marks et al., 1992; Srinivasan et al., 2011).

Compared with smokers of non-mentholated cigarettes, smokers of mentholated cigarettes have higher upregulation of α4β2-containing nAChR densities in the brain (Brody et al., 2013). There were reduced rates of smoking cessation among smokers of menthol- compared with non-menthol-containing cigarettes at both 4-week and 6-month check-ups (Gandhi et al., 2009).

There is a molecular explanation from mouse studies for the addictive properties of nanomolar range menthol treatment (Henderson et al., 2017; Henderson et al., 2016). Chronic treatment (~24 hours [hr]) with menthol alone upregulates α4 and α6 nAChR

Molecular Pharmacology Fast Forward. Published on January 22, 2019 as DOI: 10.1124/mol.118.114769
This article has not been copyedited and formatted. The final version may differ from this version.

subunits selectively in midbrain dopaminergic neurons in the ventral tegmental area (VTA) and substantia nigra pars compacta (SNc) (Henderson et al., 2016), whereas nicotine alone upregulates nAChR α4 number in GABAergic neurons of the substantia nigra pars reticulata (SNr) (Nashmi and Lester, 2007; Xiao et al., 2009). Furthermore, chronic menthol treatment alone shifted stoichiometry towards lower sensitivity $(\alpha4)_3(\beta2)_2$ and α6β2(non-β3) from higher sensitivity $(\alpha4)_2(\beta2)_3$ and α6β2β3 nAChR populations, respectively (Henderson et al., 2016). While chronic menthol treatment alone prevented nicotine reward-related behavior (Henderson et al., 2016), combined chronic menthol and nicotine treatment further enhanced reward-related behavior caused by chronic nicotine alone (Henderson et al., 2017). Additionally, chronic menthol treatment enhances nicotine-induced upregulation of α4* and α4α6* nAChR (Henderson et al., 2017).

The human α3-, α5-, β4-nAChR subunit gene cluster located on chromosome locus 15q24–25.1 is linked to the risk of nicotine dependence and smoking-associated diseases, as well as to lung cancer among smokers (Bierut et al., 2008; Chen et al., 2009; Saccone et al., 2007; Spitz et al., 2008; The Tobacco and Genetics Consortium, 2010). In a meta-analysis of 16 studies, 130 single nucleotide polymorphisms (SNPs) in 15q24–25.1 are associated with the number of cigarettes smoked a day, with rs1051730 in CHRNA3 having the strongest association (The Tobacco and Genetics Consortium, 2010). Furthermore, subunits from the α3-, α5-, β4-nAChR subunit gene cluster are expressed in the medial habenula (MhB)-interpeduncular (IPN) tract (Dineley-Miller and Patrick, 1992; Grady et al., 2009; Marks et al., 1992; Sheffield et al.,

Molecular Pharmacology Fast Forward. Published on January 22, 2019 as DOI: 10.1124/mol.118.114769
This article has not been copyedited and formatted. The final version may differ from this version.

2000; Shih et al., 2014; Whiteaker et al., 2000; Whiteaker et al., 2002), and contribute to nicotine dependence by influencing nicotine aversion in the MHb-IPN midbrain pathway (Fowler et al., 2011; Frahm et al., 2011). Compared with in patients who do not have lung cancer, α3 and β4 nAChR-encoding genes are overexpressed in small-cell lung carcinoma of lung cancer patients (Improgo et al., 2010). Agonist activation of α3β4 nAChRs can promote viability of these lung carcinoma cells, whereas antagonism or knockdown of α3β4 nAChRs reduces viability of these cells (Improgo et al., 2013).

Similar to the inhibitory effects at human α4β2 nAChRs (Hans et al., 2012), (-)-menthol, when co-applied with 30 μM ACh, is a noncompetitive antagonist at human nAChR α3β4 (IC_{50} = 100 μM), while also causing faster desensitization of ACh-evoked currents (Ton et al., 2015). It is of interest to observe chronic (~24 hr) effects of a much lower, pharmacologically relevant concentration of menthol on α3β4 nAChRs, because the estimated concentration of menthol in a smoker's brain is 0.5 – 2.5 μM (Henderson et al., 2017; Henderson et al., 2016).

We examined effects of chronic menthol (500 nM, 24 – 30 hr) treatment alone and in combination with chronic nicotine on the two potential stoichiometries, $(α3)_2(β4)_3$ and $(α3)_3(β4)_2$, and on functional plasma membrane (PM) levels of mouse α3β4 nAChRs. The efficiency of assembly and trafficking of nAChR varies depending on the receptor subtypes and the cell system in which they are expressed (Crespi et al., 2018a). These nAChRs were transiently transfected in mouse neuroblastoma-2a (Neuro-2a) cells to

Molecular Pharmacology Fast Forward. Published on January 22, 2019 as DOI: 10.1124/mol.118.114769
This article has not been copyedited and formatted. The final version may differ from this version.

determine whether α3β4 nAChRs mediate the addictive effects of menthol in mentholated cigarettes.

Molecular Pharmacology Fast Forward. Published on January 22, 2019 as DOI: 10.1124/mol.118.114769
This article has not been copyedited and formatted. The final version may differ from this version.

Materials and Methods

Reagents

(-)-Menthol (product #M2780), (±)-menthol (product #63670), (+)-menthol (product #224464), (-)-nicotine hydrogen tartrate (product #SML 1236), and acetylcholine chloride (product #A6625) were obtained from Sigma-Aldrich (St. Louis, MO).

Menthol dose selection has been discussed previously and is based on an analysis estimating the concentration of menthol in the brain following a long-term exposure paradigm, as well as on preliminary concentration-response studies (Henderson et al., 2017; Henderson et al., 2016).

Neuro-2a cell culture and transient transfection

We used mouse Neuro-2a cells (American Type Culture Collection, Manassas, VA) for our experiments. Passage 3 to 20 Neuro-2a cells (50,000) were plated onto sterilized 12-mm diameter glass coverslips (Deckgläser, Sondheim, Germany), which were placed in 35-mm culture dishes, and cultured in a humidified incubator (37°C; 95% air, 5% CO_2). Neuro-2a cells were incubated in full cell culture medium containing Eagle's minimum essential medium (EMEM), 10% fetal bovine serum (FBS), 100 units/mL of penicillin, and 100 µg/mL of streptomycin.

For both Zn^{2+}-inhibition experiments and [ACh]—response experiments (Figures 1-3 and Tables 1-3), 35-mm culture dishes containing pre-plated Neuro-2a cells were transfected with 125 ng of each nAChR subunit cDNA (mouse α3-green fluorescent

Molecular Pharmacology Fast Forward. Published on January 22, 2019 as DOI: 10.1124/mol.118.114769
This article has not been copyedited and formatted. The final version may differ from this version.

protein [GFP] and mouse wildtype [WT] β4) in the pCDNA3.1 vector. These constructs were used in (Shih et al., 2014) and contain a GFP tag within the M3-M4 loop of mouse α3 nAChR. Plasmids were mixed with 250 µl of Opti-MEM (Thermo Fisher Scientific Inc, Chino, CA) and Lipofectamine 2000 (Thermo Fisher Scientific Inc, Chino, CA) was separately mixed with 250 µl of Opti-MEM. After 5 min at 24 °C, DNA- and Lipofectamine 2000-containing Opti-MEM solutions were mixed together and incubated for 25 min at 24 °C. The solutions were then added to 35-mm culture dishes containing pre-plated Neuro-2a cells, which were then placed in the humidified incubator for 24 hr. The Opti-MEM was removed and replaced with full cell culture media containing either 500 nM (-)-menthol, 500 nM (+)-menthol, 500 nM (±)-menthol, 250 µM (-)-nicotine, combined 500 nM (-)-menthol and 250 µM (-)-nicotine, or neither menthol nor nicotine (control treatment) for 24 – 30 hr. Filter (0.2 µm)-sterilized menthol and nicotine stock solutions were used to make 500 nM menthol and/or 250 µM nicotine.

Patch-clamp electrophysiology

Neuro-2a cells were visualized with an inverted microscope (IX71, Olympus, Tokyo, Japan) and green illumination (for visualizing fluorescent proteins). Whole-cell patch-clamp techniques were used with an Axopatch 200B amplifier (Molecular Devices Axon Instruments, Sunnyvale, CA), Digidata 1440A analog-to-digital converters (Molecular Devices Axon Instruments, Sunnyvale, CA), and pClamp 10.3 software (Molecular Devices Axon Instruments, Sunnyvale, CA). Data were sampled at 10 kHz and low pass Bessel filtered at 2 kHz. Patch electrodes had a resistance of 2 – 6 MΩ when filled with intracellular solution. Series resistance (Rs) was compensated by 85 – 95% throughout

whole-cell patch-clamp recording, and data were discarded if the Rs exceeded 25 MΩ at the start or at the end of the recording.

Intracellular and extracellular solutions were used as in Henderson et al., (2016). The intracellular solution was as follows (in mM): 135 K-gluconate, 5 KCl, 5 EGTA, 0.5 $CaCl_2$, 10 HEPES, 2 Mg-ATP, and 0.1 GTP. The pH of the intracellular solution was adjusted to 7.2 with Tris-base, and osmolarity was adjusted to 298 mOsm with sucrose. Just prior to gigaseal formation, the junction potential between the patch pipette and bath solutions was nulled. Chronic menthol and/or nicotine treatments were 24 - 30 hr long and began 24 hr after transfection. All recordings were performed 47 - 58 hr following the start of transfection (average of 51.75 – 52.75 hr across all treatments, Tables 1, 2, and 3).

Acetylcholine (ACh) was dissolved in extracellular solution containing (in mM) the following: 140 NaCl, 5 KCl, 2 $CaCl_2$, 1 $MgCl_2$, 10 HEPES, and 10 glucose (280 - 320 mOsm, pH set to 7.3 with Tris-base). The 1 mM Zn^{2+} solutions were made from zinc acetate stock solutions, as in a previous study that tested Zn^{2+} sensitivity of rat α3β4 nAChR (Hsiao et al., 2001).

For both [ACh]–response and Zn^{2+}-inhibition experiments, ACh and/or 1 mM Zn^{2+} were applied by local laminar flow using an Octaflow II perfusion system (0.5 s to 5 s; 6 psi; Octaflow micromanifold tip [200 μm internal diameter] is located ~1.0 mm from Neuro-2a cell) (ALA Scientific Instruments, Farmingdale, NY) onto voltage-clamped Neuro-2a

Molecular Pharmacology Fast Forward. Published on January 22, 2019 as DOI: 10.1124/mol.118.114769
This article has not been copyedited and formatted. The final version may differ from this version.

cells (holding potential of -65 mV, after correcting for a junction potential of -16 mV). Actual current growth and decay times exceeded our calculated solution exchange time of ~18 ms, probably because of deviations from laminar-flow. Extracellular solution was perfused over the entire recording chamber at ~2.7 chamber volumes/min, while extracellular solution was also continuously perfused by local laminar-flow at 2 psi (for 30 s to 5 minutes) from the Octaflow II perfusion system when ACh and/or Zn^{2+} were not being perfused. In the experiments, the nicotine- or menthol-containing media was replaced by several washes with extracellular solution free of both nicotine and menthol, over an average period of 1.7 and 1.8 hr, respectively (minimum of 30 min). In experiments on Neuro-2a and other cultured mammalian cells, within 2 s after nicotine is removed from the extracellular solution, intracellular [nicotine] falls to undetectable levels (Shivange et al., submitted, 2019). This rules out retention of nicotine intracellularly (Jia et al., 2003). We estimate that extracellular [nicotine] or [menthol] decreased to < 1 fM. Recordings then commenced.

For [ACh]-response experiments, to avoid receptor desensitization from repetitive ACh application, we applied ACh at up to 5 min intervals. There was no statistically significant current run down in n≥4 Neuro-2a cells transfected with mouse α3-GFP β4 nAChRs with three ACh applications at (duration of ACh application): 10 μM (5 s) at 2 min intervals; 50 μM (5 s) at 3 min intervals; 100 μM (2 s) at 3 min intervals; 500 μM (1 s) at 5 min intervals; and 1000 μM (0.5 s) at 5 min intervals ($p > 0.05$, one-way ANOVA with post-hoc Tukey honestly significant difference [HSD] test). Also, current run-down caused by 1 μM ACh applied for 5 s duration was ruled out by observing no significant

Molecular Pharmacology Fast Forward. Published on January 22, 2019 as DOI: 10.1124/mol.118.114769
This article has not been copyedited and formatted. The final version may differ from this version.

difference between responses of 100 μM ACh applied 3 min before and 30 s after this 1 μM ACh application ($p > 0.05$, two-tailed t-test). Therefore, when collecting [ACh]-response data, ACh was applied at concentrations, durations, and time intervals that do not cause significant current rundown (i.e., 200 μM ACh was applied for 1 s and allowed to recover for 5 min before the next ACh application, because 500 μM ACh applied for 1 s at 5 min intervals did not cause current run down as explained earlier). Up to six out of the nine ACh concentrations (1 μM, 3 μM, 10 μM, 20 μM, 50 μM, 100 μM, 200 μM, 500 μM, and 1000 μM ACh) were applied to the cell in each recording session, and 100 μM ACh was applied twice in each recording session as a measure of current run-down. Peak current amplitudes were normalized to 1 for the maximum response for each recording session. The ACh concentrations were applied in a different order when recording at different cells. Data from different recording sessions were combined to form mean [ACh]-response curves for different chronic treatments. [ACh]-response data were fitted in Origin 2018 software (OriginLab Corportion, Northampton, MA) by:

Eq. 1

$$y = A1 + (A2 - A1)/(1 + 10\text{^}((LOGx0 - x) * p))$$

where: y = response; $A1$ = minimum response (usually near 0); $A2$ = maximum response (near to 1); p = Hill co-efficient; x = [ACh]

To compare desensitization between control and 500 nM chronic (-)-menthol treatments, we calculated the % current decay from the ACh-evoked peak at 1700 ms and 650 ms from the start of the ACh-evoked growth phase for 100 μM ACh and 200 μM ACh applications, respectively.

Molecular Pharmacology Fast Forward. Published on January 22, 2019 as DOI: 10.1124/mol.118.114769
This article has not been copyedited and formatted. The final version may differ from this version.

For Zn^{2+}-inhibition experiments, 100 μM ACh (with or without 1 mM Zn^{2+}) was applied for 1 s at 2.5 min intervals, and 1 mM Zn^{2+} and 100 μM ACh were co-applied in between 100 μM ACh only applications. Immediately prior to co-application of 1 mM Zn^{2+} and 100 μM ACh, 1 mM Zn^{2+} (without ACh) was applied to the cell for 2 s by local laminar-flow at 6 psi from the Octaflow II perfusion system. For each Zn^{2+}-inhibition experiment, there were four 100 μM ACh only applications and three 1 mM Zn^{2+} and 100 μM ACh co-applications. The % Zn^{2+}-inhibition for each experiment was calculated by:

Eq. 2

$$100 - \left[\left(\frac{x}{y}\right) * 100\right]$$

where: x = mean 100 μM ACh peak current amplitude in the presence of 1 mM Zn^{2+}, and y = mean 100 μM ACh peak current amplitude in the absence of 1 mM Zn^{2+}.

For both [ACh]-response and Zn^{2+}-inhibition experiments, data were discarded for individual recordings showing substantial current run-down (a > 2 fold difference in current amplitude evoked by 100 μM ACh applications). Neither menthol nor nicotine were present during any ACh applications in this study. The chronic nicotine and menthol treatments end at an average of 1.7 hr and 1.8 hr, respectively, before the cell was recorded.

Data analyses

Clampfit 10.3 (Molecular Devices Axon Instruments, Sunnyvale, CA) was used for analyzing peak current amplitudes. In our figures, we moved electrophysiological traces

Molecular Pharmacology Fast Forward. Published on January 22, 2019 as DOI: 10.1124/mol.118.114769
This article has not been copyedited and formatted. The final version may differ from this version.

along the time axis to account for variations in flow rates from the Octaflow manifold. Because peak inward current amplitudes of transfected α3β4 nAChRs in our dataset and published data often exceed –4 nA (Krashia et al., 2010), recorded peak current amplitudes were further corrected for underestimation due to uncompensated Rs (5 – 15%) by assuming a linear current-voltage relationship and a reversal potential of 0 mV. Uncompensated Rs was multiplied by current amplitude to calculate the shift in V_m. The shift in V_m allowed us to estimate the size of underestimated current amplitudes ([shift in V_m/holding V_m of -65 mV] X current amplitude). Bar graphs, [ACh]-response curve fitting, and average 100 μM ACh and 200 μM ACh waveforms were completed and plotted in Origin 2018 (OriginLab Corportion, Northampton, MA). We performed statistical tests (one-way ANOVA with post-hoc Tukey HSD test and two-tailed t-tests) using Origin 2018 software (OriginLab Corportion, Northampton, MA) and/or Microsoft Excel (Redmond, WA). Mean ± S.E. values are represented in bar charts, average waveforms, and tables (Figures 1-3, and Tables 1-3).

Molecular Pharmacology Fast Forward. Published on January 22, 2019 as DOI: 10.1124/mol.118.114769
This article has not been copyedited and formatted. The final version may differ from this version.

Results

Chronic menthol treatment does not alter the stoichiometry of functional mouse α3β4 nAChRs

To help understand how menthol in mentholated cigarettes may influence nicotine dependence, we studied how the functional characteristics of mouse α3β4 nAChRs are altered by chronic (24 – 30 hr) 500 nM menthol treatment. In Neuro-2a cells transiently transfected with mouse α3-GFP and β4 nAChR subunits at a 1:1 ratio, we studied whole-cell patch clamp currents. This Neuro-2a cell system has proven amenable for studies of chronic nicotine and/or chronic menthol treatment effects on α4β2 and α6β2 nAChRs (Henderson and Lester, 2015; Henderson et al., 2014; Henderson et al., 2017; Srinivasan et al., 2011; Srinivasan et al., 2012). Some clonal cell types express transfected membrane proteins at levels so high that aspects of subunit assembly, membrane tracking, and turnover become limiting, distorting regulatory processes that occur in neurons (Davila-Garcia et al., 1999; Lomazzo et al., 2011; Xiao and Kellar, 2004). Neuro-2a cells have more modest expression levels than various HEK293-derived cell lines, allowing good control of membrane proteins (Moss et al., 2009). In previous studies of Neuro-2a cells transfected with α4β2 and α6β2 nAChRs, varying the ratio of transfected subunits does affect the stoichiometry of the nAChRs (Srinivasan et al., 2012a; Fox et al., 2015); and exposure to chronic nicotine does upregulate nAChRs (Srinivasan et al., 2011; Srinivasan et al., 2012a; Srinivasan et al., 2012b; Fox et al.,

Molecular Pharmacology Fast Forward. Published on January 22, 2019 as DOI: 10.1124/mol.118.114769
This article has not been copyedited and formatted. The final version may differ from this version.

2015); and exposure to menthol alone also upregulates nAChRs (Henderson et al., 2016).

From our experiments, the EC_{50} for ACh is 99 μM (n = 6 - 13) (Figures 1A and B). Our EC_{50} is similar to the EC_{50} of 92 μM for ACh at *Xenopus* oocytes injected with mouse α3-GFP and β4 nAChR-encoding cRNAs (obtained from the same cDNA constructs used for our experiments) at a 2:3 ratio, respectively (Shih et al., 2014). Furthermore, our EC_{50} value for ACh at mouse α3-GFP and β4 nAChRs transfected in Neuro-2a cells is consistent with EC_{50} values for ACh at WT and modified mouse, rat, and human α3 and β4 nAChR encoding cRNAs injected into oocytes, as well as for human WT α3 and β4 nAChRs transfected at a 1:1 ratio in HEK293 cells (Drenan et al., 2008; Grishin et al., 2010; Krashia et al., 2010; Wang et al., 1998).

Zn^{2+}-inhibition of ACh-evoked currents at mouse α3-GFP β4 nAChRs following chronic menthol and/or nicotine treatment

Because our ACh-induced currents in transfected mouse α3β4 nAChRs and transfected human nAChRs α3β4s have similar EC_{50} values and waveforms as previously published data (Krashia et al., 2010), we hypothesized that we would find similar effects of Zn^{2+} on 100 μM ACh at mouse and human nAChRs α3β4s. We employed Zn^{2+} to assess stoichiometry. Moreover, synaptic vesicles of forebrain neurons contain Zn^{2+} (Frederickson et al., 2000). Zn^{2+} is released from neurons calcium- and depolarization-dependently, reaching estimated transient concentrations of almost 300 μM (Assaf and Chung, 1984; Howell et al., 1984).

Molecular Pharmacology Fast Forward. Published on January 22, 2019 as DOI: 10.1124/mol.118.114769
This article has not been copyedited and formatted. The final version may differ from this version.

Krashia et al. assessed the effects of Zn^{2+} on ACh-evoked currents at human α3β4 nAChRs of different stoichiometries (Krashia et al., 2010). Krashia et al. showed that a wide range of [Zn^{2+}] differentially affected the two α3β4 nAChR stoichiometries. Within this range, 1 mM Zn^{2+} actually produced opposite effects on ACh-evoked currents at the two populations, enhancing $(\alpha3)_2(\beta4)_3$ but inhibiting $(\alpha3)_3(\beta4)_2$ (Krashia et al., 2010). We therefore chose 1 mM Zn^{2+} as a sensitive way to determine mouse α3β4 nAChR stoichiometry changes by chronic drug treatments. If chronic menthol treatment (with or without co-chronic nicotine treatment) shifts towards the $(\alpha3)_3(\beta4)_2$ stoichiometry, we expect greater levels of inhibition by 1 mM Zn^{2+} compared with no chronic menthol treatment (with or without co-chronic nicotine treatment, respectively). Mazzo and colleagues found, using western blotting with co-immunoprecipitation of total cell lysates, that 1 mM nicotine treatment for 24 hr causes a shift (62%) toward $(\alpha3)_2(\beta4)_3$ from the $(\alpha3)_3(\beta4)_2$ stoichiometry in transfected HeLa cells (Mazzo et al., 2013). We used a lower concentration of 250 μM nicotine in our experiments to avoid potential non-specific effects caused by alkaline pH shifts with 1 mM nicotine. Nicotine concentrations of similar range (hundreds of μM) exist transiently in the airway surface liquid of smokers (Clunes et al., 2008; Mazzo et al., 2013); and α3β4 nAChRs may enhance the growth of lung cancers (Improgo et al., 2010; Improgo et al., 2013). Therefore, the nicotine concentration we study in our experiments has pharmacological relevance. Neither of the chronic treatments significantly changed the cell capacitance relative to control treatment ($p > 0.05$ for one-way ANOVA with post-hoc Tukey HSD test) (Table 1).

Molecular Pharmacology Fast Forward. Published on January 22, 2019 as DOI: 10.1124/mol.118.114769
This article has not been copyedited and formatted. The final version may differ from this version.

In the absence of nicotine, chronic 500 nM (-)-menthol treatment for 24 – 30 hr did not significantly alter the percentage of 1 mM Zn^{2+}-inhibition of 100 μM ACh-evoked currents compared with control treatment (no menthol and no nicotine) ($p > 0.05$ for one-way ANOVA with post-hoc Tukey HSD test, 48.5 ± 4.8% vs. 50.1 ± 6.5%, n = 16 and 14, respectively) (Figures 1C and D, Table 1). In addition, neither chronic 250 μM nicotine alone (48.7 ± 6.1%, n = 19), nor combined chronic 250 μM nicotine and 500 nM (-)-menthol (55.4 ± 5.3%, n = 20) treatments significantly altered the level of 1 mM Zn^{2+}-inhibition of 100 μM ACh-evoked current compared with control treatment ($p > 0.05$ for both treatments for one-way ANOVA with post-hoc Tukey HSD test) (Figures 1C and D, Table 1). This result indicates that compared with control treatment, neither of the chronic treatments ([-]-menthol alone, nicotine alone, or [-]-menthol and nicotine combined) changes the stoichiometry of mouse α3β4 nAChRs. Also, combined chronic 250 μM nicotine and 500 nM (-)-menthol treatment did not significantly alter the level of 1 mM Zn^{2+}-inhibition of 100 μM ACh-evoked current compared with chronic 250 μM nicotine treatment alone (55.4 ± 5.3% vs. 48.7 ± 6.1%; p,> 0.05 for one-way ANOVA with post-hoc Tukey HSD test; n = 20 and 19, respectively) (Figure 1C and D, Table 1). This result emphasizes that chronic 500 nM (-)-menthol does not influence 1 mM Zn^{2+} sensitivity of ACh-evoked currents at mouse α3β4 nAChRs. Because these control, chronically menthol-treated, and/or chronically nicotine-treated α3β4 nAChRs all showed > 45% inhibition by 1 mM Zn^{2+} (Figure 1C and D, Table 1), we suggest that most mouse α3β4 nAChRs in these transfected Neuro-2a cells possess the $(\alpha3)_3(\beta4)_2$ stoichiometry. If these α3β4 nAChRs under the different chronic treatments were predominantly in the $(\alpha3)_2(\beta4)_3$ stoichiometry, ACh-evoked currents would show

Molecular Pharmacology Fast Forward. Published on January 22, 2019 as DOI: 10.1124/mol.118.114769
This article has not been copyedited and formatted. The final version may differ from this version.

potentiation in the presence of 1 mM Zn^{2+} (Krashia et al., 2010). Our suggestion is also consistent with Krashia et al. strongly suggesting that HEK293 cells transfected with α3 and β4 nAChR subunits at a 1:1 ratio predominantly possess the $(\alpha3)_3(\beta4)_2$ stoichiometry (Krashia et al., 2010). Krashia et al. suggested this predominant $(\alpha3)_3(\beta4)_2$ stoichiometry after observing greater shifts in the EC_{50} of ACh in patch-clamp recorded transfected cells containing mutant α3 and WT β4 compared with cells containing WT α3 and mutant β4 nAChR constructs (Krashia et al., 2010).

[ACh]-response at mouse α3-GFP β4 nAChRs following chronic menthol treatment

As another experiment to probe stoichiometry changes by chronic menthol, we assessed the [ACh]-response relationship at mouse α3-GFP β4 nAChRs following chronic menthol treatment. Previous studies have shown how populations of different stoichiometry vary in the ACh EC_{50} by 2 – 3 fold at human α3β4 nAChRs (Krashia et al., 2010) and 7 – 8 fold at rat α3β4 nAChRs (Grishin et al., 2010). Because Krashia et al. (2010) found that Zn^{2+} inhibition is sensitive to α3β4 nAChR stoichiometry, our previous Zn^{2+}-inhibition experiments do present strong evidence that chronic exposure to (-)-menthol and/or nicotine fails to affect α3β4 nAChR stoichiometry. However, we recently reported that (-)-menthol and (+)-menthol have markedly different effects in chronic exposure at α4β2 nAChRs (Henderson et al., eNeuro in press, 2019). Furthermore, cigarette manufacturers could consider responding to possible governmental bans on cigarettes containing (-)-menthol (FDA, 2018), which is now the predominant isoform in mentholated cigarettes, by adding (+)-menthol instead. We therefore extended the experiments to determine whether chronic exposures to other forms of menthol [(±)-

Molecular Pharmacology Fast Forward. Published on January 22, 2019 as DOI: 10.1124/mol.118.114769
This article has not been copyedited and formatted. The final version may differ from this version.

menthol or (+)-menthol] alter α3β4 nAChR stoichiometry. Neither of the chronic menthol treatments significantly changed the cell capacitance relative to control treatment ($p > 0.05$ for one-way ANOVA with post-hoc Tukey HSD test) (Table 2).

Chronic treatments with either 500 nM (-)-menthol (EC_{50} = 134 μM; n = 5 – 12), 500 nM (±)-menthol (EC_{50} = 117 μM; n = 4 – 11), or 500 nM (+)-menthol (EC_{50} = 142 μM; n = 6 – 13) for 24 – 30 hr did not shift the EC_{50} of ACh by > 1.5 fold compared with control treatment (no menthol and no nicotine; EC_{50} = 99 μM; n = 6 – 13) at Neuro-2a cells transfected with mouse α3-GFP and WT β4 nAChR subunits (Figure 2A and B; Table 2). These [ACh]-response experiments together with the Zn^{2+}-inhibition experiments suggest that chronic menthol treatment does not shift the stoichiometry of functional mouse α3β4 nAChRs. The [ACh]-response of control and chronic menthol-treated cells have Hill slope values of between 1 – 2 (Table 2), as similarly reported in the published literature for α3β4 nAChRs (Grishin et al., 2010; Krashia et al., 2010; Shih et al., 2014). Furthermore, compared with control treatment, the different chronic menthol treatments did not significantly change the current density (pA/pF) of 100 μM ACh-evoked currents or 1 mM ACh-evoked currents ($p > 0.05$ for one-way ANOVA with post-hoc Tukey HSD test in both cases) (Table 2).

The operational definition of desensitization is a decline in agonist-induced conductance while the agonist is present. Ton et al. (2015) have previously shown that acute menthol application accelerates desensitization of currents at α3β4 nAChR by accessing the open state of the channel, and our experiments with chronic menthol treatment in the

Molecular Pharmacology Fast Forward. Published on January 22, 2019 as DOI: 10.1124/mol.118.114769
This article has not been copyedited and formatted. The final version may differ from this version.

absence of acutely applied menthol and prior to agonist activation may highlight another mechanism for modulating desensitization. We assessed effects of chronic menthol exposure on desensitization. Compared with control treatment, chronic treatment with 500 nM (-)-menthol significantly accelerated desensitization of 100 μM ACh-evoked currents at mouse α3-GFP β4 nAChRs ($p < 0.05$ for the two-tailed t-test, 39.8 ± 3.5% [n = 12] vs. 52.7 ± 5.1% [n = 12] current decay for control and chronic (-)-menthol treatment, respectively, at 1700 ms from the start of the ACh-evoked growth phase) (Figure 2C). Also, compared with control treatment, chronic treatment with 500 nM (-)-menthol significantly accelerated desensitization of 200 μM ACh-evoked currents at mouse α3-GFP β4 nAChRs ($p < 0.01$ for the two-tailed t-test, 21.6 ± 3.4% [n = 6] vs. 45.1 ± 5.7% [n = 6] current decay for control and chronic (-)-menthol treatment, respectively, at 650 ms from the start of the ACh-evoked growth phase) (Figure 2D). Our results follow the known pattern that, at higher agonist concentrations, nAChR currents desensitize more rapidly. We also tested whether, for a given ACh concentration, higher agonist-induced currents desensitize more rapidly. We pooled data for 100 μM ACh-evoked currents, and separately, for 200 μM ACh-evoked currents, for the four chronic treatments [control, (-)-menthol, (±)-menthol, and (+)-menthol], with a criterion of > 100 -pA/pF to eliminate noisy contribution from relatively small signals. We compared peak current density (-pA/pF) and % desensitization at 1700 ms and 650 ms after the start of the growth phase (for 100 μM [n = 29] and 200 μM ACh-evoked currents [n = 20], respectively). For both 100 μM ACh-evoked current and 200 μM ACh-evoked current datasets, we found no significant Pearson's correlation coefficient between peak current density and desensitization (ANOVA).

Molecular Pharmacology Fast Forward. Published on January 22, 2019 as DOI: 10.1124/mol.118.114769
This article has not been copyedited and formatted. The final version may differ from this version.

Chronic nicotine but not chronic menthol treatment reduces functional PM mouse α3β4 nAChR levels

We analyzed our dataset to assess functional PM levels of mouse α3β4 nAChRs following chronic treatments with 500 nM (-)-menthol, with 250 μM nicotine alone, with combined 250 μM nicotine and 500 nM (-)-menthol, and control (neither menthol nor nicotine). The current density (average current amplitude in pA/cell capacitance in pF) is an appropriate metric for functional PM levels of mouse α3β4 nAChR. Unlike qRT-PCR or western blot, whole-cell patch-clamp electrophysiology can reveal alterations in functional nAChR PM levels or alterations from post-translational changes. Neither of the chronic treatments in this current density analysis significantly changed the cell capacitance relative to control treatment ($p > 0.05$ for one-way ANOVA with post-hoc Tukey HSD test) (Table 3). In this section, we report on the results of t-tests as we consider the subtle differences discussed below as important findings in the field of regulation of nAChRs.

Chronic (-)-menthol treatment alone has no statistically significant effect on the current density of mouse α3β4 nAChRs compared with control treatment (no chronic nicotine nor menthol) ($p > 0.05$ for both one way-ANOVA with post-hoc Tukey HSD test and two-tailed t-test; -102.7 ± 19.6 pA/pF vs. -129.7 ± 22.9 pA/pF, n = 28 and 27, respectively) (Figure 3; Table 3). Furthermore, combined chronic (-)-menthol and nicotine treatment had no statistically significant effect on the current density of mouse α3β4 nAChRs

Molecular Pharmacology Fast Forward. Published on January 22, 2019 as DOI: 10.1124/mol.118.114769
This article has not been copyedited and formatted. The final version may differ from this version.

compared with chronic nicotine treatment alone ($p > 0.05$ for both one way-ANOVA with post-hoc Tukey HSD test and two-tailed t-test; -71.9 ± 12.3 pA/pF vs. -62.7 ± 10.4 pA/pF, n = 20 and 19, respectively) (Figure 3; Table 3). Interestingly, compared with control treatment (no chronic nicotine nor menthol), both chronic 250 μM nicotine treatment alone ($p < 0.05$ by two tailed t-test, $p > 0.05$ by one way-ANOVA; -129.7 ± 22.9 pA/pF vs. -62.7 ± 10.4 pF/pA, n = 27 and 19, respectively; 52% decrease) and combined chronic 250 μM nicotine and 500 nM menthol treatment ($p < 0.05$ by two tailed t-test, $p > 0.05$ by one way-ANOVA with post-hoc Tukey HSD test; -129.7 ± 22.9 pA/pF vs. -71.9 ± 12.3 pA/pF, n = 27 and 20, respectively; 45% decrease) caused a reduction in the current density of mouse α3β4 nAChRs (Figure 3; Table 3). Therefore, chronic nicotine treatment at 250 μM causes a reduction in functional mouse α3β4 nAChR PM levels in Neuro-2a cells. Because we extensively washed the nicotine (250 μM) for ≥ 30 min, and usually 100 min, in nicotine-free extracellular solution before the recording session (see Materials and Methods) for that cell, no classically defined “desensitization” process would adequately describe the reduced function.

Molecular Pharmacology Fast Forward. Published on January 22, 2019 as DOI: 10.1124/mol.118.114769
This article has not been copyedited and formatted. The final version may differ from this version.

Discussion

We undertook these experiments to understand whether chronic exposure to sub-μM menthol alters the properties of α3β4 nAChRs, whose abundance in the MhB-IPN pathway may dominate the aversive properties of nicotine. The pharmacokinetics of menthol in humans have proven challenging to study, presumably because menthol is glucuronidated via first-pass metabolism (Gelal et al., 1999), but we have estimated elsewhere that menthol concentrations in the brain of a mouse model of smoking to be 0.5 – 2.5 μM (Henderson et al., 2017; Henderson et al., 2016).

Long-term pharmacological effects on PM levels of nAChRs proceed, at least in part, via differential trafficking of the major subunit stoichiometries, $\alpha_2\beta_3$ vs. $\alpha_3\beta_2$. Therefore, we sought to measure both subunit stoichiometry and PM nAChR levels. Chronic (24 – 30 hr) menthol treatment at 500 nM neither significantly altered subunit stoichiometry [$(\alpha3)_2(\beta4)_3$ vs. $(\alpha3)_3(\beta4)_2$] on the PM nor significantly changed functionally measured PM protein levels of mouse nAChR α3β4 ($p > 0.05$ for both).

Faced with this insensitivity to chronic menthol, we sought to know whether chronic nicotine itself affects either functional PM stoichiometry or functional PM protein levels in mouse α3β4 nAChR levels in the Neuro-2a cell assay system. Surprisingly, chronic nicotine at a concentration many times that found in the blood following smoking decreased rather than increased the current density of 100 μM ACh-evoked currents, indicating reduced functional mouse α3β4 PM protein levels.

Molecular Pharmacology Fast Forward. Published on January 22, 2019 as DOI: 10.1124/mol.118.114769
This article has not been copyedited and formatted. The final version may differ from this version.

The β subunit is probably the dominant factor causing the contrast between chronic nicotine and/or menthol effects on α4β2 and α6β2, vs. on α3β4. In our assay system, α4β4 nAChRs are exported efficiently from the ER to the PM; most α4β2 nAChRs are not (Richards et al., 2011; Srinivasan et al., 2011). That is, in the absence of nicotine, mouse α4β4 nAChRs are already highly distributed in the PM relative to the ER. Previous experiments show a mechanistic basis for this difference. The mouse nAChR β4 subunit has an ER export motif (LXM), but no ER retention motif (RRQR), and these properties explain how mouse α3β4 nAChRs efficiently exit the ER to reach the PM (Mazzo et al., 2013; Srinivasan et al., 2011). Indeed, the crucial interaction may occur at the single previously non-binding β subunit, also termed “accessory” (Crespi et al., 2018b). Mouse α4-eGFP β2 nAChRs with modified β2 subunits containing an export motif and without the ER retention motif were strongly localized to the PM relative to the ER (2.36 fold increase in PM-integrated density over mouse α4-eGFP WT β2 nAChRs), and chronic (48 hr) nicotine at 100 nM treatment caused only a modest (1.2 fold) additional increase in the PM integrated density (Srinivasan et al., 2011). Chronic (48 hr) nicotine at 100 nM upregulated mouse α4-GFP WT β2 nAChRs more substantially (1.9 fold increase in PM-integrated density) (Srinivasan et al., 2011). The export motif is absent in both the nAChR α3 subunit and in the mouse nAChR β2 subunit, while the mouse nAChR β4 subunit contains an ER export motif (Mazzo et al., 2013; Srinivasan et al., 2011). Therefore, it is mechanistically understandable how mouse nAChR α3β4 nAChRs have a high PM vs. ER distribution without additional aids to ER export of α3β4 nAChRs.

Molecular Pharmacology Fast Forward. Published on January 22, 2019 as DOI: 10.1124/mol.118.114769
This article has not been copyedited and formatted. The final version may differ from this version.

What is the relevance to chronic effects of menthol? Previous experiments show that chronic sub-μM menthol also apparently acts in the early exocytotic pathway to aid the ER exit of nAChRs (Henderson et al., 2017; Henderson et al., 2016). The observed details of chronic menthol effects differ from those of chronic nicotine effects, and probably also from the acute blocking effects of menthol at [menthol] > 100-fold higher than our chronically applied concentrations (Ton et al., 2015). We tentatively suggested that chronic sub-μM menthol could act as a nonspecific "chemical chaperone" for α4β2 and α6β2 nAChRs (Henderson et al., 2016); but the target could also be another protein in the early exocytotic pathway. In any case, because α3β4 nAChRs do not experience a rate-limiting step in the early exocytotic pathway due to the absence of an ER retention motif, it is mechanistically understandable that menthol treatment causes no further increase in the already high existing PM vs. ER distribution.

Certain more subtle effects of chronic sub-μM menthol cannot be ruled out. Chronic 500 nM (-)-menthol treatment accelerated desensitization of ACh-evoked currents at mouse α3β4 nAChRs, even > 1 hr after we washed out the menthol. This effect is unlikely to arise from a menthol-nAChR binding with a lifetime of ~1 hr. We can also rule out sequelae of (-)-menthol interactions with TRPM8, the classical menthol target, because Neuro-2a cells do not express TRPM8 mRNA (Henderson et al., 2016). However, phosphorylation of nAChRs does, in some cases, enhance desensitization (Di Angelantonio et al., 2011; Hopfield et al., 1988; Huganir et al., 1986; Nishizaki and Sumikawa, 1998). Whether an unknown pathway activates protein kinase(s) during

Molecular Pharmacology Fast Forward. Published on January 22, 2019 as DOI: 10.1124/mol.118.114769
This article has not been copyedited and formatted. The final version may differ from this version.

chronic exposure to 500 nM (-)-menthol, and whether nAChR phosphorylation is stable for > 1 hr after the menthol is removed, cannot be evaluated at present.

The steps leading to functional α3β4 nAChRs reaching the cell membrane include: 1) assembly of subunits into a pentamer; and 2) post-assembly trafficking, which can be affected by degradation of the pentamer. While our experiments and previously published data indicate that α3 and β4 subunits preferentially assemble into a $(\alpha3)_3(\beta4)_2$ stoiochiometry (Krashia et al., 2010), this stoichiometry is still prone to degradation (Mazzo et al., 2013). Therefore, our patch-clamp experiments mainly record currents from the $(\alpha3)_3(\beta4)_2$ stoichiometry because the $(\alpha3)_2(\beta4)_3$ stoichiometry may reach the plasma membrane less efficiently due to possibly lower pentamer assembly. Additional intracellular $(\alpha3)_3(\beta4)_2$ complexes formed in the presence of chronic menthol may undergo degradation before they can be trafficked to the PM. Preliminary data from our laboratory lend support to such a mechanism, but at higher menthol concentrations than used here (Patowary et al., 2016).

Mechanism of downregulation by chronic nicotine

Previous experiments indicate that chronic treatments with nicotine have less dramatic effects on protein levels of nAChR α3β4 compared with nAChR α4β2 in several brain regions studied (Davila-Garcia et al., 2003; Fox et al., 2015; Marks et al., 2015; Meyer et al., 2001; Nguyen et al., 2003; Wang et al., 1998). In a contrasting report, chronic (14 days) nicotine treatment in rats caused downregulation of nAChR α3β4-like binding sites in the subiculum and cerebellum (Nguyen et al., 2003). Although efficient

membrane trafficking usually limits the PM levels of α3β4 nAChRs, Mazzo and colleagues skillfully rendered membrane tracking the rate-limiting step, by inhibiting protein synthesis with cycloheximide. Under these circumstances, nicotine-induced upregulation of human α3β4 nAChRs occurs through the increased stability of the $(\alpha3)_2(\beta4)_3$ stoichiometry (Mazzo et al., 2013), leading to increased trafficking to the PM. It is unlikely that chronic nicotine treatment would cause decreased current density of 100 μM ACh-evoked currents through a shift towards the lower potency mouse $(\alpha3)_3(\beta4)_2$ nAChR stoichiometry, because 1) when Neuro-2a cells in our study or HEK293 cells in another study were transfected with α3 and β4 nAChRs at a 1:1 ratio, the level of Zn^{2+}-inhibition of ACh-evoked currents suggests $(\alpha3)_3(\beta4)_2$ as the predominant stoichiometry (Krashia et al., 2010); 2) if nicotine shifts α3β4 nAChR stoichiometry, it would be towards $(\alpha3)_2(\beta4)_3$ (Mazzo et al., 2013), as nicotine shifting towards a stoichiometry of three α and two β subunits of any nAChR has not been previously reported.

Our finding, that nicotine-induced downregulation of mouse α3β4 nAChRs, is not common but recalls experiments on other nAChRs. In toxin binding studies in rodents or primates, nicotine downregulates α6* nAChRs in some cases (Lai et al., 2005; McCallum et al., 2006b; Mugnaini et al., 2006) but not others (McCallum et al., 2006a; Visanji et al., 2006), and the effect depends on the detailed stoichiometry of the complex (Fox et al., 2015; Perez et al., 2008).

Further question and conclusions

Molecular Pharmacology Fast Forward. Published on January 22, 2019 as DOI: 10.1124/mol.118.114769
This article has not been copyedited and formatted. The final version may differ from this version.

It will be interesting to study whether chronic menthol treatment has different effects at α3β4 vs. α3β4α5 nAChRs, analogous to the differential modulation by lynx1 of human α3β4 and α3β4α5 nAChRs (George et al., 2017). Furthermore, functional α3β4β3 nAChRs are present in brain (Grady et al., 2009). It remains possible that the subunit in the "accessory position" influences the nature of the subunit interfaces (Walsh et al., 2018) and hence potentially the effects from chronic treatments by menthol or other chaperones.

In conclusion, chronic menthol treatment (500 nM, 24 – 30 hr) failed to shift the [ACh]-response relationship and Zn^{2+} sensitivity of ACh-evoked currents at mouse α3β4 nAChRs, suggesting no change in receptor stoichiometry at the PM. Furthermore, compared with no drug treatment, the current density of 100 ACh-evoked currents was not significantly changed following chronic menthol treatment ($p > 0.05$), indicating that functional mouse α3β4 nAChR PM levels were not changed. Mechanistically, these data are broadly consistent with the view that chronic effects of sub-μM menthol act via events in the early exocytotic pathway. Pathopharmacologically, our datasets suggest that smoking mentholated cigarettes, which enhances smoking addiction and nicotine addiction, exerts these effects via mechanisms other than chronic sub-μM exposure of α3β4 nAChRs.

Molecular Pharmacology Fast Forward. Published on January 22, 2019 as DOI: 10.1124/mol.118.114769
This article has not been copyedited and formatted. The final version may differ from this version.

Acknowledgements

We are grateful to Suparna Patowary for performing preliminary experiments on chronic menthol treatment effects at mouse α3β4 nAChRs (Patowary et al., 2016).

Author Contributions

Participated in research design: Bavan, Henderson, and Lester.

Conducted experiments: Bavan and Kim.

Contributed new reagents or analytic tools: not applicable.

Performed data analysis: Bavan, Henderson, and Lester.

Wrote or contributed to the writing of the manuscript: Bavan, Kim, Henderson, and Lester.

References

Assaf SY and Chung SH (1984) Release of endogenous Zn^{2+} from brain tissue during activity. *Nature* **308**(5961): 734-736.

Bierut LJ, Stitzel JA, Wang JC, Hinrichs AL, Grucza RA, Xuei X, Saccone NL, Saccone SF, Bertelsen S, Fox L, Horton WJ, Breslau N, Budde J, Cloninger CR, Dick DM, Foroud T, Hatsukami D, Hesselbrock V, Johnson EO, Kramer J, Kuperman S, Madden PA, Mayo K, Nurnberger J, Jr., Pomerleau O, Porjesz B, Reyes O, Schuckit M, Swan G, Tischfield JA, Edenberg HJ, Rice JP and Goate AM (2008) Variants in nicotinic receptors and risk for nicotine dependence. *Am J Psychiatry* **165**(9): 1163-1171.

Brody AL, Mukhin AG, La Charite J, Ta K, Farahi J, Sugar CA, Mamoun MS, Vellios E, Archie M, Kozman M, Phuong J, Arlorio F and Mandelkern MA (2013) Up-regulation of nicotinic acetylcholine receptors in menthol cigarette smokers. *Int J Neuropsychopharmacol* **16**(5): 957-966.

Buisson B and Bertrand D (2001) Chronic exposure to nicotine upregulates the human α4β2 nicotinic acetylcholine receptor function. *J Neurosci* **21**(6): 1819-1829.

CDC (2018) Fast Facts.

Chen X, Chen J, Williamson VS, An SS, Hettema JM, Aggen SH, Neale MC and Kendler KS (2009) Variants in nicotinic acetylcholine receptors α5 and α3 increase risks to nicotine dependence. *Am J Med Genet B Neuropsychiatr Genet* **150B**(7): 926-933.

Clunes LA, Bridges A, Alexis N and Tarran R (2008) *In vivo* versus *in vitro* airway surface liquid nicotine levels following cigarette smoke exposure. *J Anal Toxicol* **32**(3): 201-207.

Crespi A, Colombo SF and Gotti C (2018a) Proteins and chemical chaperones involved in neuronal nicotinic receptor expression and function: an update. *Br J Pharmacol* **175**(11): 1869-1879.

Crespi A, Plutino S, Sciaccaluga M, Righi M, Borgese N, Fucile S, Gotti C and Colombo SF (2018b) The fifth subunit in α3β4 nicotinic receptor is more than an accessory subunit. *FASEB journal : official publication of the Federation of American Societies for Experimental Biology* **32**(8): 4190-4202.

Davila-Garcia MI, Houghtling RA, Qasba SS and Kellar KJ (1999) Nicotinic receptor binding sites in rat primary neuronal cells in culture: characterization and their regulation by chronic nicotine. *Brain Res Mol Brain Res* **66**(1-2): 14-23.

Davila-Garcia MI, Musachio JL and Kellar KJ (2003) Chronic nicotine administration does not increase nicotinic receptors labeled by [^{125}I]epibatidine in adrenal gland, superior cervical ganglia, pineal or retina. *J Neurochem* **85**(5): 1237-1246.

Di Angelantonio S, Piccioni A, Moriconi C, Trettel F, Cristalli G, Grassi F and Limatola C (2011) Adenosine A2A receptor induces protein kinase A-dependent functional modulation of humanα α3β4 nicotinic receptor. *J Physiol* **589**(Pt 11): 2755-2766.

Dineley-Miller K and Patrick J (1992) Gene transcripts for the nicotinic acetylcholine receptor subunit, β4, are distributed in multiple areas of the rat central nervous system. *Brain Res Mol Brain Res* **16**(3-4): 339-344.

Drenan RM, Nashmi R, Imoukhuede PI, Just H, McKinney S and Lester HA (2008) Subcellular Trafficking, Pentameric Assembly and Subunit Stoichiometry of Neuronal Nicotinic ACh Receptors Containing Fluorescently-Labeled α6 and β3 Subunits. *Mol Pharmacol* **73**: 27-41.

FDA (2018) Statement from FDA Commissioner Scott Gottlieb, M.D., on proposed new steps to protect youth by preventing access to flavored tobacco products and banning menthol in cigarettes.

Flores CM, Rogers SW, Pabreza LA, Wolfe BB and Kellar KJ (1992) A subtype of nicotinic cholinergic receptor in rat-brain is composed of α4 subunit and β2-subunit and is up-regulated by chronic nicotine treatment. *Mol Pharmacol* **41**: 31-37.

Fowler CD, Lu Q, Johnson PM, Marks MJ and Kenny PJ (2011) Habenular α5 nicotinic receptor subunit signalling controls nicotine intake. *Nature* **471**: 597-601.

Fox AM, Moonschi FH and Richards CI (2015) The nicotine metabolite, cotinine, alters the assembly and trafficking of a subset of nicotinic acetylcholine receptors. *J Biol Chem* **290**(40): 24403-24412.

Frahm S, Slimak MA, Ferrarese L, Santos-Torres J, Antolin-Fontes B, Auer S, Filkin S, Pons S, Fontaine JF, Tsetlin V, Maskos U and Ibanez-Tallon I (2011) Aversion to nicotine is regulated by the balanced activity of β4 and α5 nicotinic receptor subunits in the medial habenula. *Neuron* **70**(3): 522-535.

Frederickson CJ, Suh SW, Silva D, Frederickson CJ and Thompson RB (2000) Importance of zinc in the central nervous system: the zinc-containing neuron. *J Nutr* **130**(5S Suppl): 1471S-1483S.

Gandhi KK, Foulds J, Steinberg MB, Lu SE and Williams JM (2009) Lower quit rates among African American and Latino menthol cigarette smokers at a tobacco treatment clinic. *Int J Clin Pract* **63**(3): 360-367.

Gelal A, Jacob P, 3rd, Yu L and Benowitz NL (1999) Disposition kinetics and effects of menthol. *Clin Pharmacol Ther* **66**(2): 128-135.

George AA, Bloy A, Miwa JM, Lindstrom JM, Lukas RJ and Whiteaker P (2017) Isoform-specific mechanisms of α3β4*-nicotinic acetylcholine receptor modulation by the prototoxin lynx1. *FASEB journal : official publication of the Federation of American Societies for Experimental Biology* **31**(4): 1398-1420.

Grady SR, Moretti M, Zoli M, Marks MJ, Zanardi A, Pucci L, Clementi F and Gotti C (2009) Rodent habenulo-interpeduncular pathway expresses a large variety of uncommon nAChR subtypes, but only the α3β4* and α3β3β4* subtypes mediate acetylcholine release. *J Neurosci* **29**(7): 2272-2282.

Grishin AA, Wang CI, Muttenthaler M, Alewood PF, Lewis RJ and Adams DJ (2010) α-conotoxin AuIB isomers exhibit distinct inhibitory mechanisms and differential sensitivity to stoichiometry of α3β4 nicotinic acetylcholine receptors. *J Biol Chem* **285**(29): 22254-22263.

Hans M, Wilhelm M and Swandulla D (2012) Menthol suppresses nicotinic acetylcholine receptor functioning in sensory neurons via allosteric modulation. *Chemical senses* **37**(5): 463-469.

Henderson BJ and Lester HA (2015) Inside-out neuropharmacology of nicotinic drugs. *Neuropharmacol* **96**(Pt B): 178-193.

Henderson BJ, Srinivasan R, Nichols WA, Dilworth CN, Gutierrez DF, Mackey ED, McKinney S, Drenan RM, Richards CI and Lester HA (2014) Nicotine exploits a COPI-mediated process for chaperone-mediated up-regulation of its receptors. *J Gen Physiol* **143**(1): 51-66.

Henderson BJ, Wall TR, Henley BM, Kim CH, McKinney S and Lester HA (2017) Menthol Enhances Nicotine Reward-Related Behavior by Potentiating Nicotine-Induced Changes in nAChR Function, nAChR Upregulation, and DA Neuron Excitability. *Neuropsychopharmacology* **42**(12): 2285-2291.

Henderson BJ, Wall TR, Henley BM, Kim CH, Nichols WA, Moaddel R, Xiao C and Lester HA (2016) Menthol Alone Upregulates Midbrain nAChRs, Alters nAChR Subtype Stoichiometry, Alters Dopamine Neuron Firing Frequency, and Prevents Nicotine Reward. *J Neurosci* **36**(10): 2957-2974.

Henderson et al., eNeuro in press (2019) Henderson, BJ, Grant S, Chu BW, Shahoei R, Huard SM, Saladi SSM, Tajkhorshid E, Dougherty DA, and Lester HA. Menthol stereoisomers exhibit different effects on α4β2 nAChR upregulation and dopamine neuron spontaneous firing.

Hopfield JF, Tank DW, Greengard P and Huganir RL (1988) Functional modulation of the nicotinic acetylcholine-receptor by tyrosine phosphorylation. *Nature* **336**: 677-680.

Howell GA, Welch MG and Frederickson CJ (1984) Stimulation-induced uptake and release of zinc in hippocampal slices. *Nature* **308**(5961): 736-738.

Hsiao B, Dweck D and Luetje CW (2001) Subunit-dependent modulation of neuronal nicotinic receptors by zinc. *J Neurosci* **21**(6): 1848-1856.

Huganir RL, Delcour AH, Greengard P and Hess GP (1986) Phosphorylation of the nicotinic acetylcholine receptor regulates its rate of desensitization. *Nature* **321**(6072): 774-776.

Improgo MR, Schlichting NA, Cortes RY, Zhao-Shea R, Tapper AR and Gardner PD (2010) ASCL1 regulates the expression of the CHRNA5/A3/B4 lung cancer susceptibility locus. *Mol Cancer Res* **8**(2): 194-203.

Improgo MR, Soll LG, Tapper AR and Gardner PD (2013) Nicotinic acetylcholine receptors mediate lung cancer growth. *Front Physiol* **4**: 251.

Jia L, Flotildes K, Li M and Cohen BN (2003) Nicotine trapping causes the persistent desensitization of α4β2 nicotinic receptors expressed in oocytes. *J Neurochem* **84**(4): 753-766.

Krashia P, Moroni M, Broadbent S, Hofmann G, Kracun S, Beato M, Groot-Kormelink PJ and Sivilotti LG (2010) Human α3β4 neuronal nicotinic receptors show different stoichiometry if they are expressed in *Xenopus* oocytes or mammalian HEK293 cells. *PLoS One* **5**(10): e13611.

Lai A, Parameswaran N, Khwaja M, Whiteaker P, Lindstrom JM, Fan H, McIntosh JM, Grady SR and Quik M (2005) Long-term nicotine treatment decreases striatal α6* nicotinic acetylcholine receptor sites and function in mice. *Mol Pharmacol* **67**(5): 1639-1647.

Lomazzo E, Hussmann GP, Wolfe BB, Yasuda RP, Perry DC and Kellar KJ (2011) Effects of chronic nicotine on heteromeric neuronal nicotinic receptors in rat primary cultured neurons. *J Neurochem* **119**(1): 153-164.

Marks MJ, O'Neill HC, Wynalda-Camozzi KM, Ortiz NC, Simmons EE, Short CA, Butt CM, McIntosh JM and Grady SR (2015) Chronic treatment with varenicline changes expression of four nAChR binding sites in mice. *Neuropharmacology* **99**: 142-155.

Marks MJ, Pauly JR, Gross SD, Deneris ES, Hermans-Borgmeyer I, Heinemann SF and Collins AC (1992) Nicotine binding and nicotinic receptor subunit RNA after chronic nicotine treatment. *J Neurosci* **12**(7): 2765-2784.

Mazzo F, Pistillo F, Grazioso G, Clementi F, Borgese N, Gotti C and Colombo SF (2013) Nicotine-Modulated Subunit Stoichiometry Affects Stability and Trafficking of α3β4 Nicotinic Receptor. *J Neurosci* **33**(30): 12316-12328.

McCallum SE, Parameswaran N, Bordia T, Fan H, McIntosh JM and Quik M (2006a) Differential regulation of mesolimbic α3*/α6*β2 and α4*β2 nicotinic acetylcholine receptor sites and function after long-term oral nicotine to monkeys. *J Pharmacol Exp Ther* **318**(1): 381-388.

McCallum SE, Parameswaran N, Bordia T, Fan H, Tyndale RF, Langston JW, McIntosh JM and Quik M (2006b) Increases in α4* but not α3*/α6* nicotinic receptor sites and function in the primate striatum following chronic oral nicotine treatment. *J Neurochem* **96**(4): 1028-1041.

Meyer EL, Xiao Y and Kellar KJ (2001) Agonist regulation of rat α3β4 nicotinic acetylcholine receptors stably expressed in human embryonic kidney 293 cells. *Mol Pharmacol* **60**(3): 568-576.

Moss FJ, Imoukhuede PI, Scott K, Hu J, Jankowsky JL, Quick MW and Lester HA (2009) GABA transporter function, oligomerization state, and anchoring: correlates with subcellularly resolved FRET. *J Gen Physiol* **134**(6): 489-521.

Mugnaini M, Garzotti M, Sartori I, Pilla M, Repeto P, Heidbreder CA and Tessari M (2006) Selective down-regulation of [^{125}I]Y_0- α-conotoxin MII binding in rat mesostriatal dopamine pathway following continuous infusion of nicotine. *Neuroscience* **137**(2): 565-572.

Nashmi R and Lester H (2007) Cell autonomy, receptor autonomy, and thermodynamics in nicotine receptor up-regulation. *Biochem Pharmacol* **74**(8): 1145-1154.

Nguyen HN, Rasmussen BA and Perry DC (2003) Subtype-selective up-regulation by chronic nicotine of high-affinity nicotinic receptors in rat brain demonstrated by receptor autoradiography. *J Pharmacol Exp Ther* **307**(3): 1090-1097.

Nishizaki T and Sumikawa K (1998) Effects of PKC and PKA phosphorylation on desensitization of nicotinic acetylcholine receptors. *Brain Res* **812**(1-2): 242-245.

Patowary S, Mackey EDW, McKinney SL, Deshpande P, Henderson BJ, Biener G, Raicu V and Lester HA (2016) Effects of Menthol on α3β4* Nicotinic Receptors. *Biophysical Journal* **110**(3): 603A-603A.

Perez XA, Bordia T, McIntosh JM, Grady SR and Quik M (2008) Long-term nicotine treatment differentially regulates striatal α6α4β2* and α6(Nonα4)β2* nAChR expression and function. *Mol Pharmacol* **74**(3): 844-853.

Richards CI, Srinivasan R, Xiao C, Mackey ED, Miwa JM and Lester HA (2011) Trafficking of α4* nicotinic receptors revealed by superecliptic phluorin: effects of

a β4 amyotrophic lateral sclerosis-associated mutation and chronic exposure to nicotine. *J Biol Chem* **286**(36): 31241-31249.

Saccone SF, Hinrichs AL, Saccone NL, Chase GA, Konvicka K, Madden PA, Breslau N, Johnson EO, Hatsukami D, Pomerleau O, Swan GE, Goate AM, Rutter J, Bertelsen S, Fox L, Fugman D, Martin NG, Montgomery GW, Wang JC, Ballinger DG, Rice JP and Bierut LJ (2007) Cholinergic nicotinic receptor genes implicated in a nicotine dependence association study targeting 348 candidate genes with 3713 SNPs. *Hum Mol Genet* **16**(1): 36-49.

Sheffield EB, Quick MW and Lester RA (2000) Nicotinic acetylcholine receptor subunit mRNA expression and channel function in medial habenula neurons. *Neuropharmacology* **39**(13): 2591-2603.

Shih PY, Engle SE, Oh G, Deshpande P, Puskar NL, Lester HA and Drenan RM (2014) Differential expression and function of nicotinic acetylcholine receptors in subdivisions of medial habenula. *J Neurosci* **34**(29): 9789-9802.

Shivange et al., submitted (2019) Shivange A, Borden P, Muthusamy A, Nichols A, Bera K, Bao H, Bishara I, Jeon J, Mulcahy M, Cohen B, O'Riordan S, Kim C, Dougherty D, Chapman E, Marvin J, Looger L and Lester H (2018) Nicotinic Drugs in the Endoplasmic Reticulum: Beginning the Inside-out Pathway of Addiction and Therapy. *J Gen Physiol* **submitted**.

Spitz MR, Amos CI, Dong Q, Lin J and Wu X (2008) The CHRNA5-A3 region on chromosome 15q24-25.1 is a risk factor both for nicotine dependence and for lung cancer. *J Natl Cancer Inst* **100**(21): 1552-1556.

Srinivasan R, Pantoja R, Moss FJ, Mackey EDW, Son C, Miwa J and Lester HA (2011) Nicotine upregulates α4β2 nicotinic receptors and ER exit sites via stoichiometry-dependent chaperoning. *J Gen Physiol* **137**: 59-79.

Srinivasan R, Richards CI, Dilworth C, Moss FJ, Dougherty DA and Lester HA (2012a) Forster resonance energy transfer (FRET) correlates of altered subunit stoichiometry in cys-loop receptors, exemplified by nicotinic α4β2. *Int J Mol Sci* **13**(8): 10022-10040.

Srinivasan R, Richards CI, Xiao C, Rhee D, Pantoja R, Dougherty DA, Miwa JM and Lester HA (2012b) Pharmacological chaperoning of nicotinic acetylcholine receptors reduces the endoplasmic reticulum stress response. *Mol Pharmacol* **81**(6): 759-769.

The Tobacco and Genetics Consortium (2010) Genome-wide meta-analyses identify multiple loci associated with smoking behavior. *Nat Genet* **42**(5): 441-447

Ton HT, Smart AE, Aguilar BL, Olson TT, Kellar KJ and Ahern GP (2015) Menthol Enhances the Desensitization of Human α3β4 Nicotinic Acetylcholine Receptors. *Mol Pharmacol* **88**(2): 256-264.

Visanji NP, Mitchell SN, O'Neill MJ and Duty S (2006) Chronic pre-treatment with nicotine enhances nicotine-evoked striatal dopamine release and α6 and β3 nicotinic acetylcholine receptor subunit mRNA in the substantia nigra pars compacta of the rat. *Neuropharmacology* **50**(1): 36-46.

Walsh RM, Jr., Roh SH, Gharpure A, Morales-Perez CL, Teng J and Hibbs RE (2018) Structural principles of distinct assemblies of the human α4β2 nicotinic receptor. *Nature* **557**(7704): 261-265.

Wang F, Nelson ME, Kuryatov A, Olale F, Cooper J, Keyser K and Lindstrom J (1998) Chronic nicotine treatment up-regulates human α3β2 but not α3β4 acetylcholine receptors stably transfected in human embryonic kidney cells. *J Biol Chem* **273**(44): 28721-28732.

Whiteaker P, McIntosh JM, Luo S, Collins AC and Marks MJ (2000) [^{125}I]-α-conotoxin MII identifies a novel nicotinic acetylcholine receptor population in mouse brain. *Mol Pharmacol* **57**(5): 913-925.

Whiteaker P, Peterson CG, Xu W, McIntosh JM, Paylor R, Beaudet AL, Collins AC and Marks MJ (2002) Involvement of the α3 subunit in central nicotinic binding populations. *J Neurosci* **22**(7): 2522-2529.

WHO (2015) WHO global report on trends in prevalence of tobacco smoking.

Xiao C, Nashmi R, McKinney S, Cai H, McIntosh JM and Lester HA (2009) Chronic nicotine selectively enhances α4β2* nicotinic acetylcholine receptors in the nigrostriatal dopamine pathway. *J Neurosci* **29**: 12428-12439.

Xiao Y and Kellar KJ (2004) The comparative pharmacology and up-regulation of rat neuronal nicotinic receptor subtype binding sites stably expressed in transfected mammalian cells. *J Pharmacol Exp Ther* **310**(1): 98-107.

Molecular Pharmacology Fast Forward. Published on January 22, 2019 as DOI: 10.1124/mol.118.114769
This article has not been copyedited and formatted. The final version may differ from this version.

Footnotes

This study was supported by National Institutes of Health [Grants DA037743, DA046335, and DA036061].

Molecular Pharmacology Fast Forward. Published on January 22, 2019 as DOI: 10.1124/mol.118.114769
This article has not been copyedited and formatted. The final version may differ from this version.

Figure legends

Figure 1.

Functional characterization shows that chronic (24 – 30 hr) (-)-menthol and/or nicotine treatment does not change the Zn^{2+} sensitivity of ACh-evoked currents at mouse α3β4 nAChRs. cDNA-encoding mouse α3-GFP and WT β4 subunits were transfected at a 1:1 ratio into Neuro-2a cells. Using whole-cell patch clamp at a holding potential -65 mV, inward current responses were recorded during ACh application at the indicated concentrations and the chronic treatment conditions are underlined. Menthol and/or nicotine were not present during ACh application. **A,** [ACh]-response curves (average normalized response ± S.E. values are represented in the curve) were constructed (n = 6 – 13 for different concentrations). **B,** exemplar voltage-clamp current traces displayed by their ACh concentration and duration of application. **C,** Chronic 500 nM (-)-menthol (n = 16), chronic 250 μM nicotine (n = 19), and combined chronic 500 nM (-)-menthol and 250 μM nicotine treatments (n = 20) did not significantly (n.s.) change the level of inhibition of 100 μM ACh by 1 mM Zn^{2+} compared with control treatment (n = 14) ($p > 0.05$ for both one-way ANOVA with post-hoc Tukey HSD test and two-tailed t-tests). Mean ± S.E. values are represented in the bar chart. The 1 mM Zn^{2+} solution without ACh was applied to the Neuro-2a cells for 2 s before it was co-applied with 100 μM ACh for 1 s. **D,** Exemplar traces of 100 μM ACh only application 2.5 min before, during co-application, and 100 μM ACh only application 2.5 min after (washout) 100 μM ACh + 1 mM Zn^{2+} co-application (Zn^{2+} co-app.). The black bar represents ACh application for all 3 traces, and the adjoining grey bar represents ACh for 1-2 traces (differences in

Molecular Pharmacology Fast Forward. Published on January 22, 2019 as DOI: 10.1124/mol.118.114769
This article has not been copyedited and formatted. The final version may differ from this version.

application due to the variations in flow rates from the Octaflow manifold that combined solutions).

Figure 2.

Chronic (24 – 30 hr) menthol treatment does not shift the [ACh]-response relationship at mouse α3β4 nAChRs transfected into Neuro-2a cells, but accelerates desensitization kinetics. Menthol and/or nicotine were not present during ACh application. Chronic treatments key: control = black; (-)-menthol = green; (±)-menthol = blue; (+)-menthol = purple. **A,** [ACh]-response curves (average normalized response ± S.E. values are represented in the curves) were constructed for chronic treatments with 500 nM (-)-menthol, 500 nM (+)-menthol, 500 nM (±)-menthol (n = 5 – 12, 6 – 13, and 4 – 11, respectively for the different concentrations) and plotted with control (no menthol, n = 6-13, as in Figure 1). EC_{50} values in Table 2. **B,** exemplar traces from chronic 500 nM (-)-menthol treatment displayed by their ACh concentration and duration of application**. C, D,** chronic menthol treatment alters desensitization of 100 μM **(C)** and 200 μM **(D)** ACh-evoked currents. The % current decay from the ACh-evoked peak was calculated at 1700 ms 650 ms from the start of the ACh-evoked growth phase for 100 μM ACh and 200 μM ACh applications, respectively. Mean current waveform curves with standard error for no drug-treated, (-)-menthol, (+)-menthol, and (±)-menthol treated chronically at transfected Neuro-2a cells (average of 12, 12, 11, and 13 cells for 100 μM ACh [C], and average of 6, 6, 5, and 6 and 200 μM ACh [D], respectively). Mean ± S.E. values are represented in the waveforms in C and D.

Molecular Pharmacology Fast Forward. Published on January 22, 2019 as DOI: 10.1124/mol.118.114769
This article has not been copyedited and formatted. The final version may differ from this version.

Figure 3.

Chronic (24 – 30 hr) (-)-menthol treatment does not alter functional PM levels of mouse α3β4 nAChRs transiently transfected into Neuro-2a cells. Summary of current density (-pA/pF) for the different chronic treatments (control, 500 nM (-)-menthol, 250 μM nicotine, and combined 500 nM (-)-menthol and 250 μM nicotine; n = 27, 28, 19, and 20, respectively). n.s., not significantly changed ($p > 0.05$) by one-way ANOVA with post-hoc Tukey HSD test. Mean ± S.E. values are represented in the bar chart. Menthol and/or nicotine were not present during ACh application.

Molecular Pharmacology Fast Forward. Published on January 22, 2019 as DOI: 10.1124/mol.118.114769
This article has not been copyedited and formatted. The final version may differ from this version.

TABLE 1. Level (%) of 1 mM Zn^{2+}-inhibition of 100 μM ACh-currents at mouse α3β4 nAChRs under different chronic (24 – 30 hr) treatments. Cells were studied 52.5 – 52.75 hr after transfection and 26.5 – 27.25 hr after incubation in no drug-containing media or after menthol and/or nicotine was added (both durations are averages).

Chronic treatment	**Control**	**(-)-menthol**	**Nicotine**	**Nicotine and (-)-menthol**
(-)-Menthol (nM)	0	500	0	500
Nicotine (μM)	0	0	250	250
% Zn^{2+}-inhibition[a]	50.1 ± 6.5	48.5 ± 4.8	48.7 ± 6.1	55.4 ± 5.3
N	14	16	19	20
Cell capacitance (pF)[a]	28.2 ± 5.3	23.3 ± 2.5	22.5 ± 1.9	22.9 ± 1.9
Current density (pA/pF)[a, b]	-108.4 ± 31.6	-91.4 ± 15.6	-62.7 ± 10.4	-71.9 ± 12.3

Mean ± S.E. values are represented in the table

[a]$p > 0.05$ for one way-ANOVA with post-hoc Tukey HSD test

[b]Current density between these same chronic treatments with higher N numbers for control and chronic (-)-menthol treatment are shown in Table 3 and discussed in the Results section entitled 'Chronic nicotine but not chronic menthol treatment reduces functional PM mouse α3β4 nAChR levels'

Molecular Pharmacology Fast Forward. Published on January 22, 2019 as DOI: 10.1124/mol.118.114769
This article has not been copyedited and formatted. The final version may differ from this version.

TABLE 2. [ACh]-response at mouse α3β4 nAChRs under different chronic (24 – 30 hr) treatments. Cells were studied 51.75 – 52.75 hr after transfection and 25.75 – 26.5 hr after incubation in no drug-containing media or after menthol was added (both durations are averages).

Chronic treatment	**Control**	**(-)-menthol**	**(±)-menthol**	**(+)-menthol**
N	6 – 13	5 – 12	4 – 11	6 – 13
EC_{50} (μM)	99 ± 14	134 ± 18	117 ± 16	142 ± 5
Hill slope	1.14 ± 0.18	1.42 ± 0.24	1.28 ± 0.21	1.59 ± 0.07
Cell capacitance (pF)[a]	19.7 ± 1.9	20.0 ± 3.7	17.6 ± 2.0	16.0 ± 1.9
Current density (pA/pF) of 100 μM ACh currents[a]	-153.2 ± 33.3	-117.1 ± 41.4	-196.9 ± 42.9	-214.5 ± 33.4
Current density (pA/pF) of 1 mM ACh currents[a]	-363.1 ± 84.6	-295.9 ± 86.7	-440.5 ± 64.1	-566.1 ± 84.4

Mean ± S.E. values are represented in the table

[a]$p > 0.05$ for one way-ANOVA with post-hoc Tukey HSD test

Molecular Pharmacology Fast Forward. Published on January 22, 2019 as DOI: 10.1124/mol.118.114769
This article has not been copyedited and formatted. The final version may differ from this version.

TABLE 3. Current density (pA/pF) at mouse α3β4 nAChRs under different chronic (24 – 30 hr) treatments. Cells were studied 52.5 – 52.75 hr after transfection and 26.5 – 27.0 hr after incubation in no drug-containing media or after menthol and/or nicotine was added (both durations are averages).

Chronic treatment	**Control**	**(-)-menthol**	**Nicotine**	**Nicotine and (-)-menthol**
(-)-Menthol (nM)	0	500	0	500
Nicotine (μM)	0	0	250	250
Cell capacitance (pF)[a]	24.1 ± 3.0	21.9 ± 2.1	22.5 ± 1.9	22.9 ± 1.9
Current density (pF/pA)[a]	-129.7 ± 22.9	-102.7 ± 19.6	-62.7 ± 10.4	-71.9 ± 12.3
N	27	28	19	20

Mean ± S.E. values are represented in the table

[a]$p > 0.05$ for one way-ANOVA with post-hoc Tukey HSD test

Molecular Pharmacology Fast Forward. Published on January 22, 2019 as DOI: 10.1124/mol.118.114769
This article has not been copyedited and formatted. The final version may differ from this version.

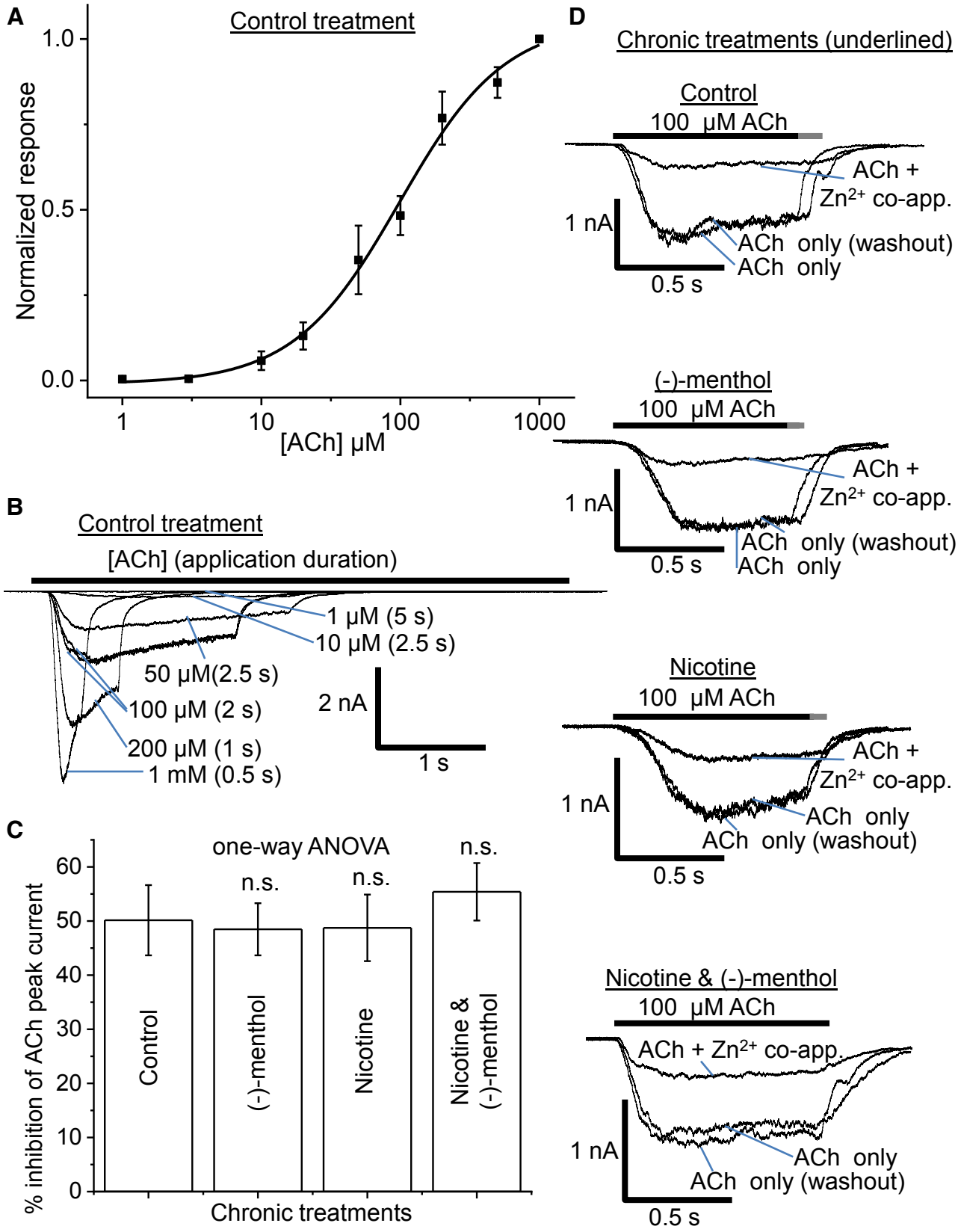

Figure 1

Molecular Pharmacology Fast Forward. Published on January 22, 2019 as DOI: 10.1124/mol.118.114769
This article has not been copyedited and formatted. The final version may differ from this version.

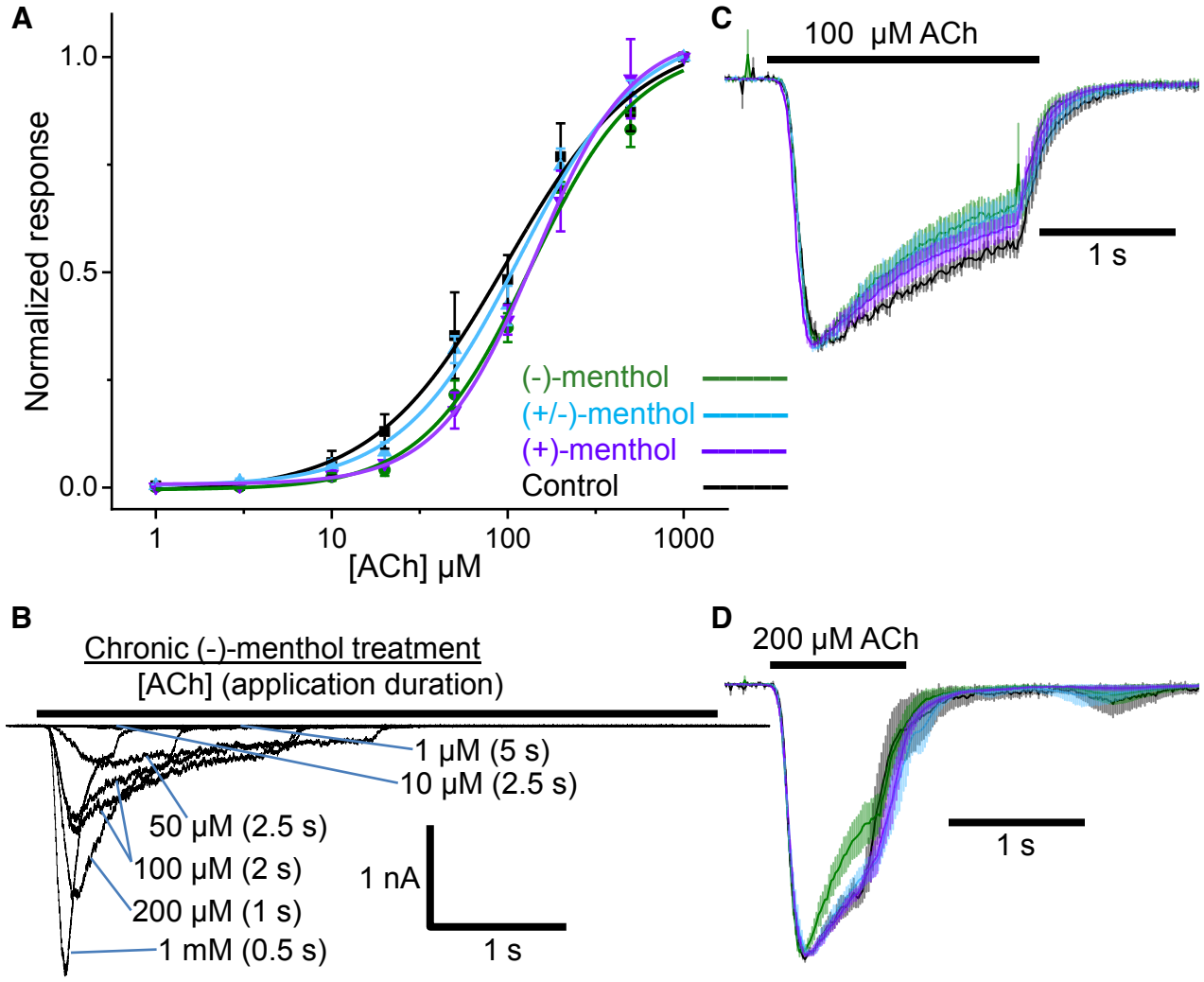

Figure 2

Molecular Pharmacology Fast Forward. Published on January 22, 2019 as DOI: 10.1124/mol.118.114769
This article has not been copyedited and formatted. The final version may differ from this version.

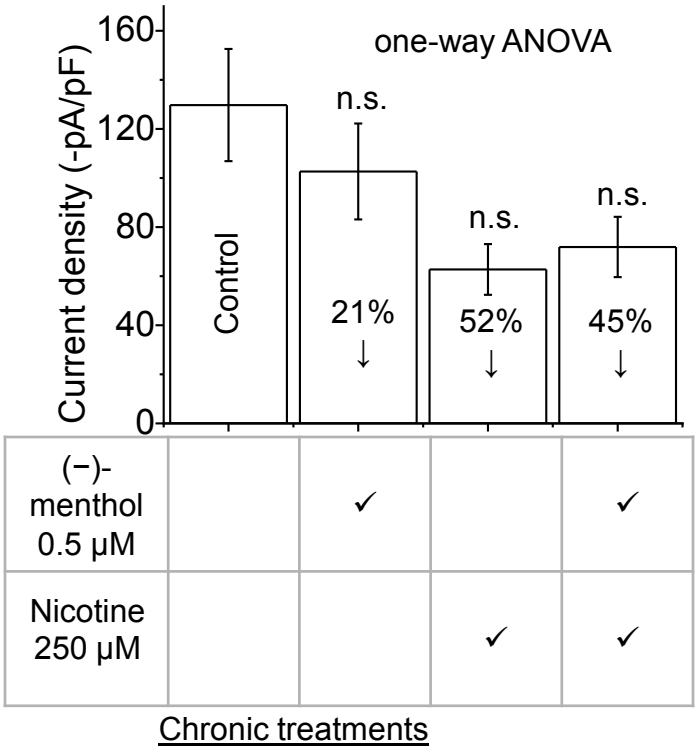

Figure 3